nature biotechnology

SUPPLEMENTARY INFORMATION

https://doi.org/10.1038/s41587-020-0492-5

In the format provided by the authors and unedited.

Generation of pancreatic β cells from CD177$^+$ anterior definitive endoderm

Pallavi U. Mahaddalkar[1,2,8], Katharina Scheibner[1,8], Sandra Pfluger[1], Ansarullah[1], Michael Sterr[1,2], Julia Beckenbauer[1], Martin Irmler[3], Johannes Beckers[3,4,5], Sebastian Knöbel[6] and Heiko Lickert[1,2,5,7] ✉

---

[1]Institute of Diabetes and Regeneration Research, Helmholtz Diabetes Center, Helmholtz Zentrum München, Neuherberg, Germany. [2]Institute of Stem Cell Research, Helmholtz Zentrum München, Neuherberg, Germany. [3]Institute of Experimental Genetics, Helmholtz Zentrum München, Neuherberg, Germany. [4]Chair of Experimental Genetics, School of Life Sciences Weihenstephan, Technische Universität München, Freising, Germany. [5]German Center for Diabetes Research (DZD), Neuherberg, Germany. [6]Miltenyi Biotec, Bergisch Gladbach, Germany. [7]β-Cell Biology, Technische Universität München, School of Medicine, Klinikum Rechts der Isar, Munich, Germany. [8]These authors contributed equally: Pallavi U. Mahaddalkar, Katharina Scheibner.
✉e-mail: heiko.lickert@helmholtz-muenchen.de

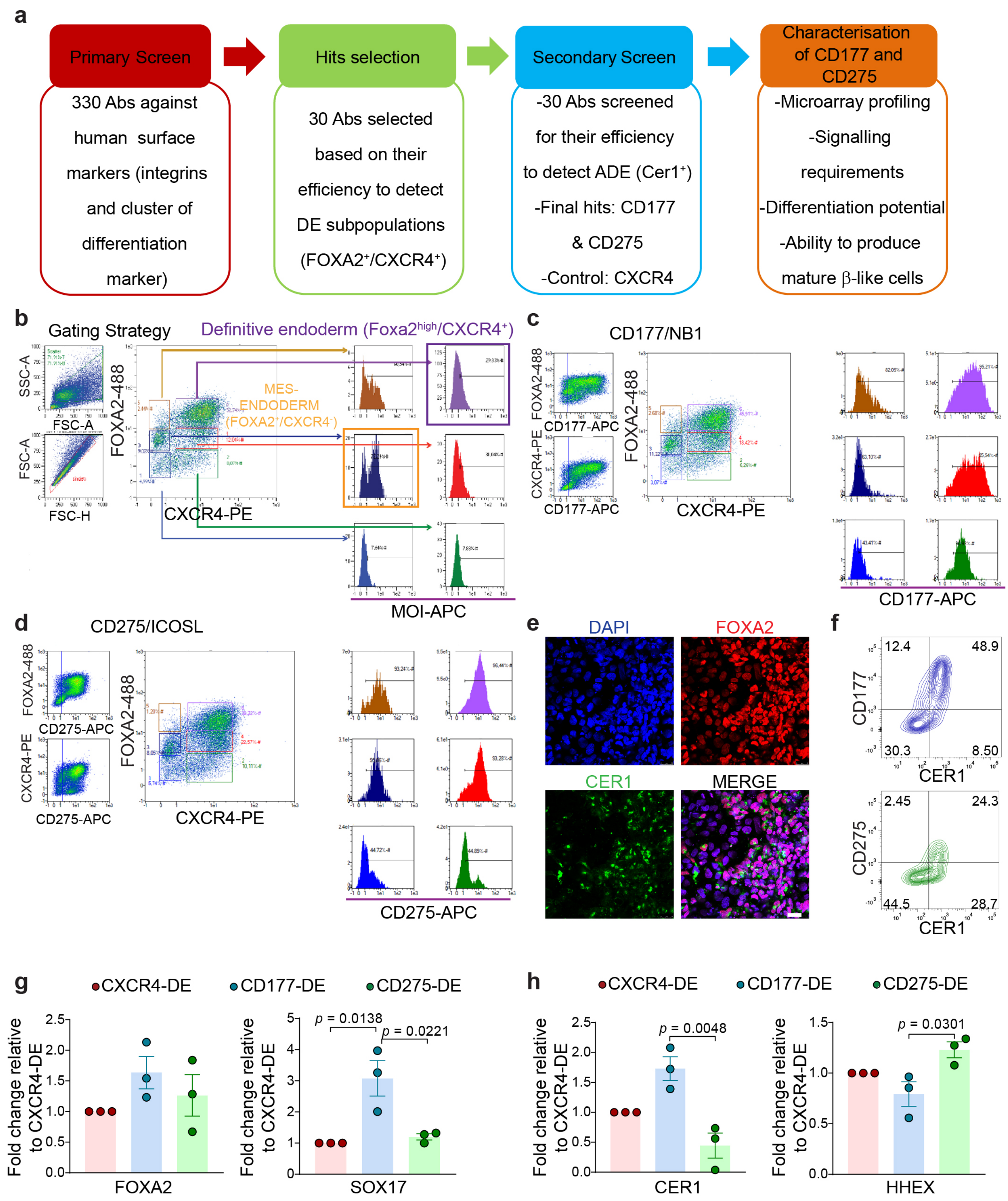

Supplementary Figure 1

Screening strategy for the identification of endoderm subpopulations

(a) Screening work flow for the initial screen. (b-d) Representative FACS plots for CD177 and CD275 (b) labelling of differentiated day 4 DE cells with known endoderm markers (FOXA2 and CXCR4) revealed definitive endoderm ($FOXA2^+/CXCR4^+$) and mes-endoderm ($FOXA2^{low}/CXCR4^-$) subpopulations. (c-d) CD177 and CD275 expression profiles reveal different endoderm subpopulations (*n* = 1). (e) Immunofluorescent staining for CER1 with FOXA2 in DE cultures (*n* = 3, biologically independent experiments). Scale bar, 25 µm. (f) FACS analysis for $CD275^+/CER1^+$ and $CD177^+/CER1^+$ ADE cell populations at day 4 DE. (g-h) qPCR quantification for the mRNA expression of FOXA2 and SOX17 (g), CER1 and HHEX (h) in enriched $CD177^+$ and $CD275^+$ ADE subpopulations (ANOVA, (e-h) *n* = 3, biologically independent experiments). Data is represented as mean ±s.e.m; $P<0.05$ and $P<0.01$. Statistically non-significant results are not indicated in the figure.

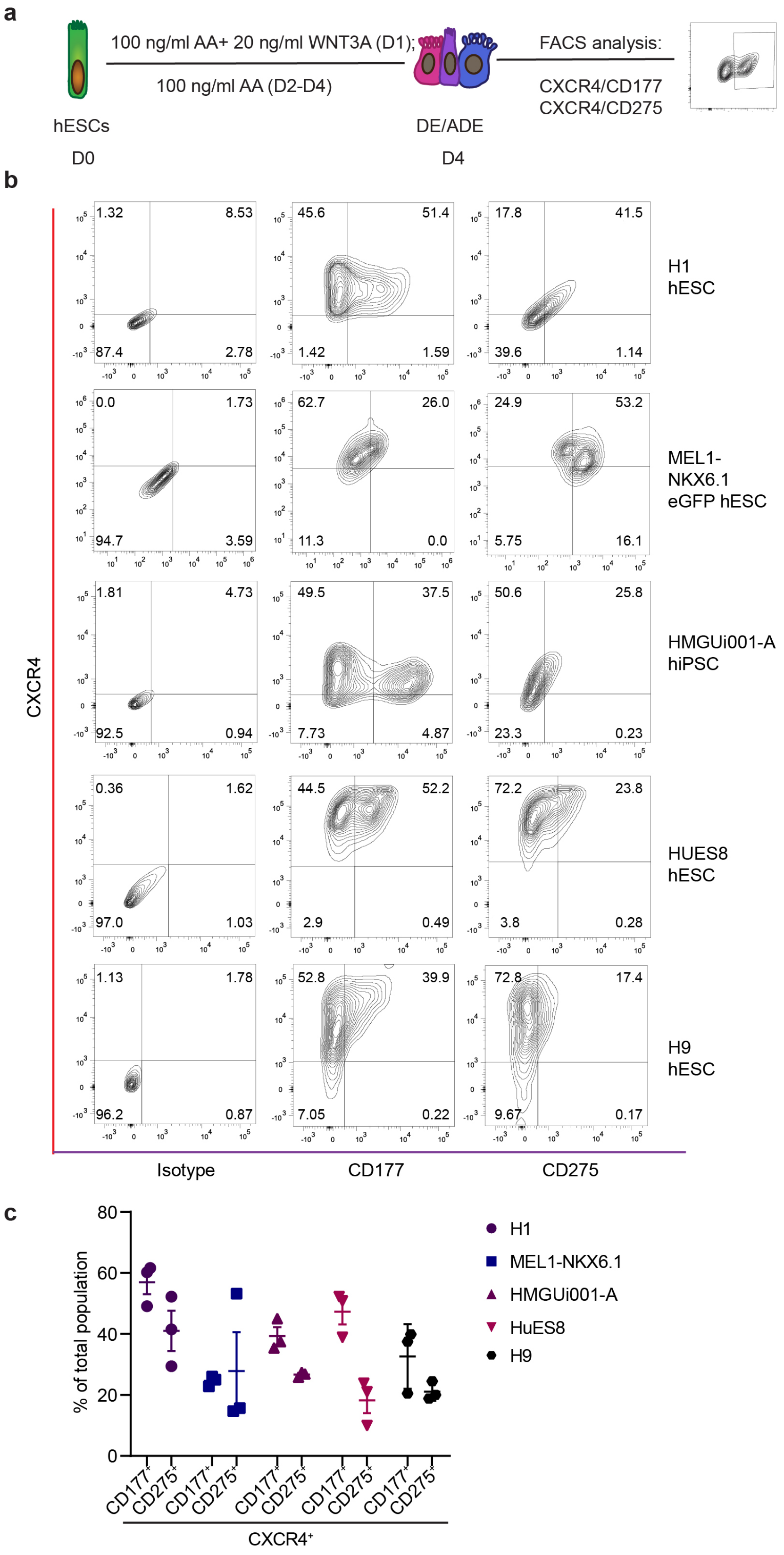
a
100 ng/ml AA+ 20 ng/ml WNT3A (D1);
100 ng/ml AA (D2-D4)
hESCs
D0
DE/ADE
D4
FACS analysis:
CXCR4/CD177
CXCR4/CD275
b
CXCR4
1.32 8.53 87.4 2.78
45.6 51.4 1.42 1.59
17.8 41.5 39.6 1.14
H1
hESC
0.0 1.73 94.7 3.59
62.7 26.0 11.3 0.0
24.9 53.2 5.75 16.1
MEL1-
NKX6.1
eGFP hESC
1.81 4.73 92.5 0.94
49.5 37.5 7.73 4.87
50.6 25.8 23.3 0.23
HMGUi001-A
hiPSC
0.36 1.62 97.0 1.03
44.5 52.2 2.9 0.49
72.2 23.8 3.8 0.28
HUES8
hESC
1.13 1.78 96.2 0.87
52.8 39.9 7.05 0.22
72.8 17.4 9.67 0.17
H9
hESC
Isotype
CD177
CD275
c
% of total population
80
60
40
20
0
CD177⁺ CD275⁺ CD177⁺ CD275⁺ CD177⁺ CD275⁺ CD177⁺ CD275⁺ CD177⁺ CD275⁺
CXCR4⁺
● H1
■ MEL1-NKX6.1
▲ HMGUi001-A
▼ HuES8
● H9

Supplementary Figure 2

Percentage of CD177$^+$ and CD275$^+$ ADE subpopulations induced in different hESC and hiPSC lines

(a) Endoderm differentiation scheme from hESCs toward DE/ADE. (b) FACS plots represent the percentage of CXCR4$^+$/CD177$^+$ and CXCR4$^+$/CD275$^+$ subpopulations in hH1, hMEL1-NKX6.1, HMGUi001-A hiPSC, HUES8 and H9 at DE/ADE stage. (c) Quantification of flow cytometry data from ((b,c) *n* = 3, biologically independent experiments).

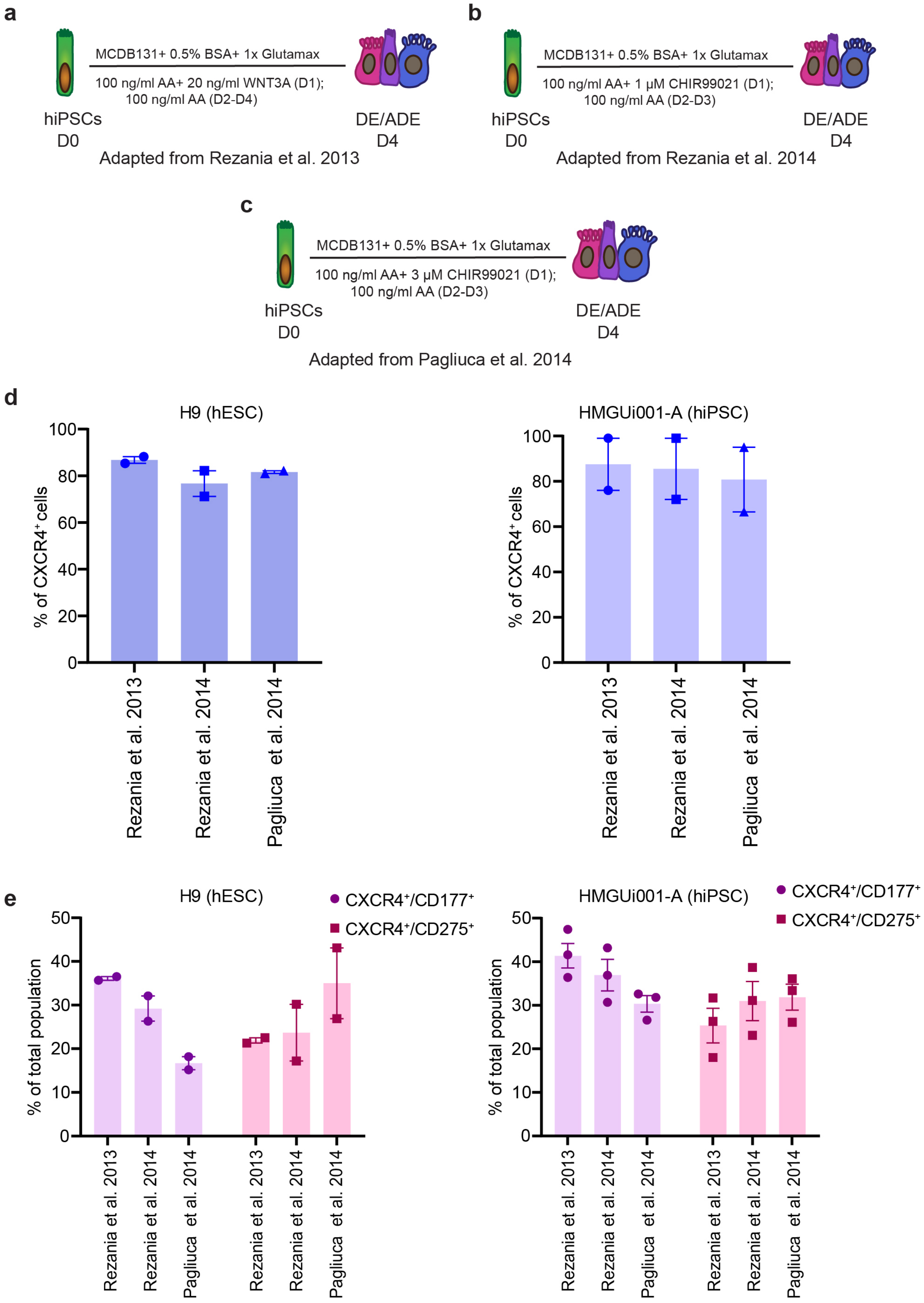
a
MCDB131+ 0.5% BSA+ 1x Glutamax
100 ng/ml AA+ 20 ng/ml WNT3A (D1);
100 ng/ml AA (D2-D4)
hiPSCs
D0
DE/ADE
D4
Adapted from Rezania et al. 2013
b
MCDB131+ 0.5% BSA+ 1x Glutamax
100 ng/ml AA+ 1 μM CHIR99021 (D1);
100 ng/ml AA (D2-D3)
hiPSCs
D0
DE/ADE
D4
Adapted from Rezania et al. 2014
c
MCDB131+ 0.5% BSA+ 1x Glutamax
100 ng/ml AA+ 3 μM CHIR99021 (D1);
100 ng/ml AA (D2-D3)
hiPSCs
D0
DE/ADE
D4
Adapted from Pagliuca et al. 2014
d
H9 (hESC)
% of CXCR4⁺ cells
0
20
40
60
80
100
Rezania et al. 2013
Rezania et al. 2014
Pagliuca et al. 2014
HMGUi001-A (hiPSC)
% of CXCR4⁺ cells
0
20
40
60
80
100
Rezania et al. 2013
Rezania et al. 2014
Pagliuca et al. 2014
e
H9 (hESC)
● CXCR4⁺/CD177⁺
■ CXCR4⁺/CD275⁺
% of total population
0
10
20
30
40
50
Rezania et al. 2013
Rezania et al. 2014
Pagliuca et al. 2014
Rezania et al. 2013
Rezania et al. 2014
Pagliuca et al. 2014
HMGUi001-A (hiPSC)
● CXCR4⁺/CD177⁺
■ CXCR4⁺/CD275⁺
% of total population
0
10
20
30
40
50
Rezania et al. 2013
Rezania et al. 2014
Pagliuca et al. 2014
Rezania et al. 2013
Rezania et al. 2014
Pagliuca et al. 2014

Supplementary Figure 3

Induction efficiency of CD177^{+} and CD275^{+} ADE shows variation using different protocols

(a-c) Adaptation of previously published endoderm differentiation protocols from hESCs. (d) FACS quantification for the percentage of total population expressing CXCR4 in DE cells derived from HMGUi001-A hiPSC using 3 different endoderm induction protocols (*n* = 2 biologically independent experiments). (e) FACS quantification for the percentage of cells expressing CXCR4^{+}/CD177^{+} and CXCR4^{+}/CD275^{+} in DE generated using previously published protocols (*n* = 3 (HMGUi001-A hiPSC), *n* = 2 (H9) biologically independent experiments). Data is represented as mean ±s.e.m.

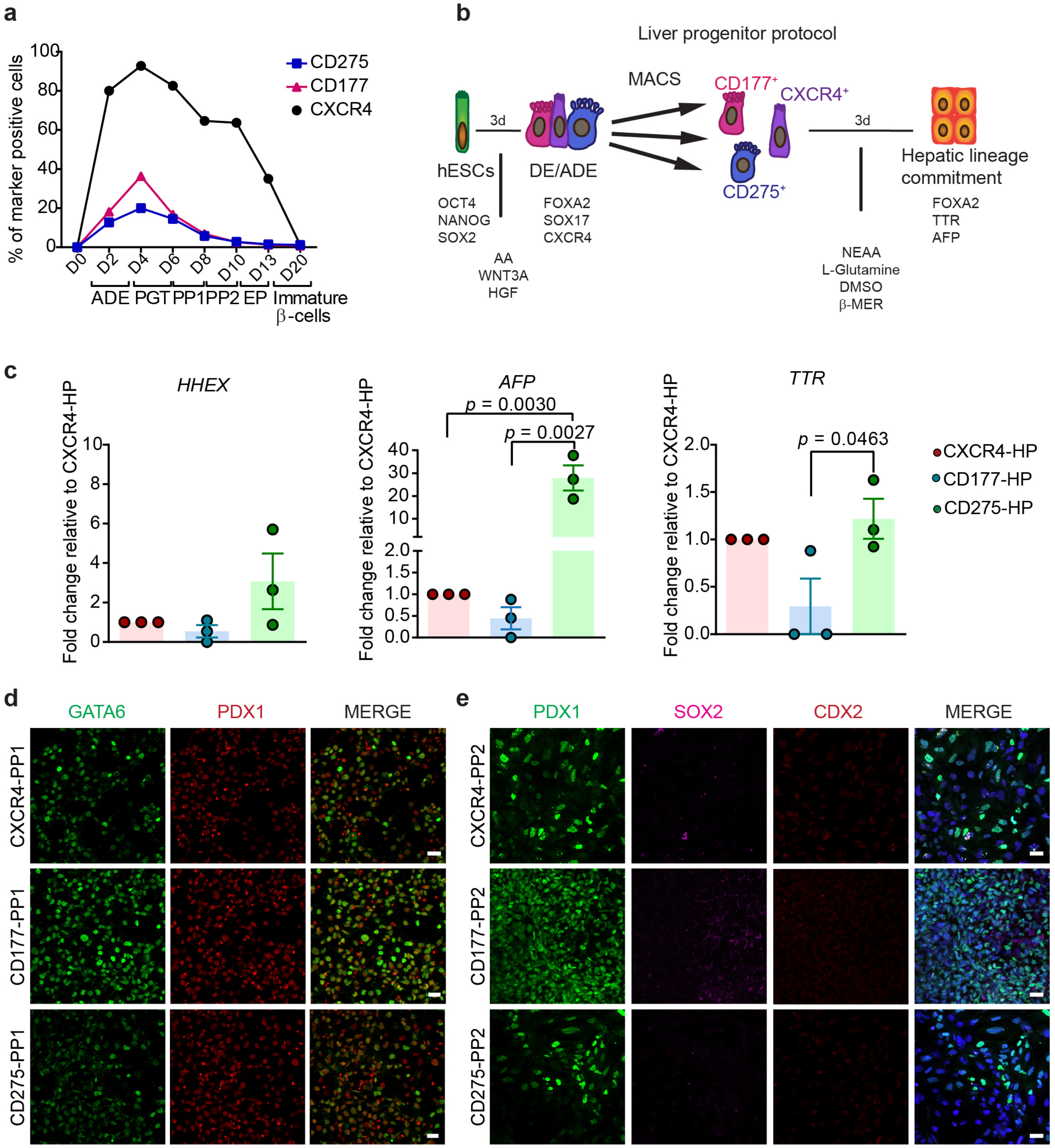

Supplementary Figure 4

Differentiation of enriched CD177$^+$, CD275$^+$ and CXCR4$^+$ ADE subpopulations toward liver and pancreas fate

(a) Expression of CD177-, CD275-, and CXCR4 during differentiation of hESCs toward pancreatic β-like cells. (b) Liver differentiation protocol. (c) qPCR quantification of the expression of early liver progenitor markers *HHEX, TTR* and *AFP* in enriched ADE subpopulations (ANOVA, *n* = 3, biologically independent experiments). (d) Immunofluorescent staining of pancreatic progenitor cells derived from enriched ADE subpopulations for the co-expression of posterior foregut marker GATA6 and PDX1. (e) Immunofluorescent staining of pancreatic progenitor cells derived from enriched ADE subpopulations for the co-expression of lung marker SOX2, intestinal marker CDX2 and PDX1 ((d, e) $n = 3$, biologically independent experiments). Data is represented as mean ±s.e.m; $P<0.05$ and $P<0.01$. Statistically non-significant results are not indicated in the figure. Scale bars, 25μm.

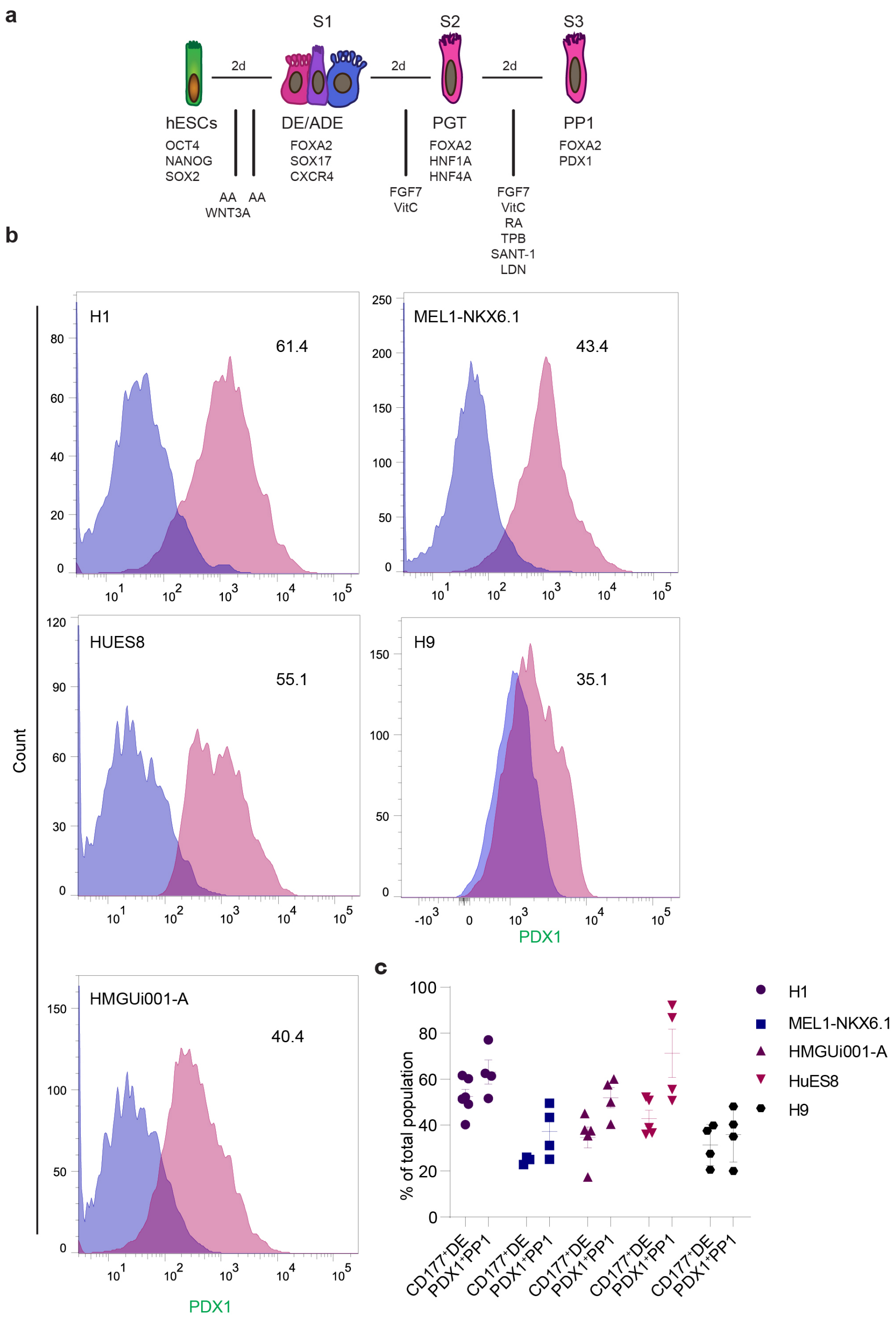

Supplementary Figure 5

CD177$^+$ ADE positively correlates with PP1 induction

(a) Pancreatic induction protocol. (b) FACS analysis of H1, HMGUi001-A hiPSC, HUES8 and MEL1-NKX6.1 for PDX1 at S3 stage. (c) Quantification of CD177$^+$ cells generated at S1 and PDX1$^+$ cells generated at S3 stage showing correlation between CD177 and PDX1 induction (*n* = 10 (H1), *n* = 7 (MEL1-NKX6.1), *n* = 9 (HMGUi001-A), *n* = 9 (HuES8), *n* = 8 (H9)). Data is represented as mean ±s.e.m.

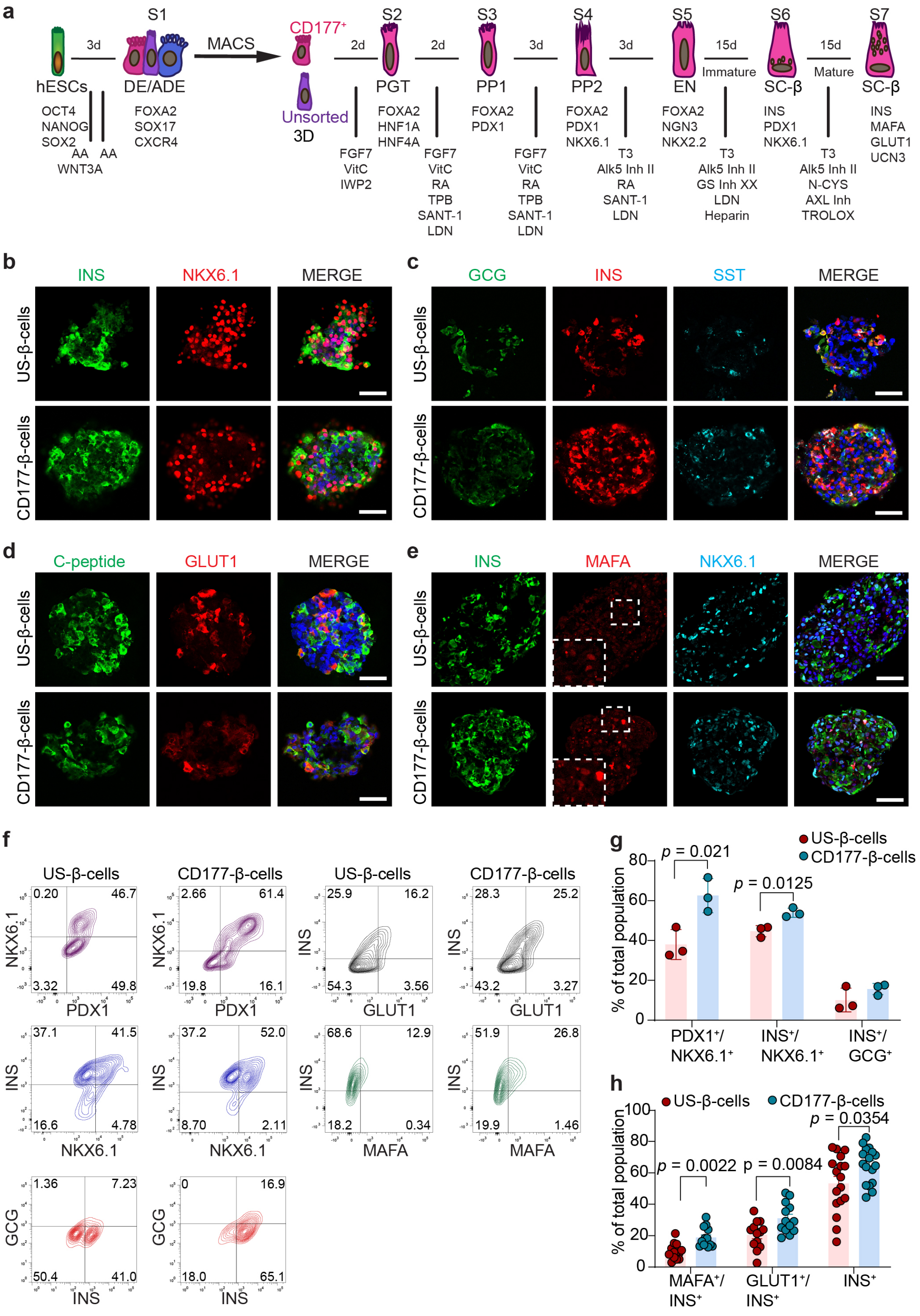

Supplementary Figure 6

H1 hESC pancreatic and endocrine differentiations of CD177$^+$- and US-DE

(a) Overview of differentiation protocol used to generate CD177-/US-β-cells. (b-e) Immunostainings for INS and NKX6.1 (b), GCG, INS and SST (c) and C-peptide and GLUT1 (d), INS, MAFA and NKX6.1 (e) in CD177- and US- β-cells ((b-e) n = 3, biologically independent experiments). Scale bars, 50 µm. (f) Representative flow cytometry contour plots of S4 and S7 cells generated from CD177$^+$- and US-ADE/DE cells on H1 line and stained for indicated markers. (g,h) Percentage of cells expressing indicated markers (two-sided unpaired Student's t-test, (g) n = 3, (h) n=13, n = 17 for INS+, biologically independent experiments). Data is represented as mean ±s.e.m; $P<0.05$ and $P<0.01$. Statistically non-significant results are not indicated in the figure.

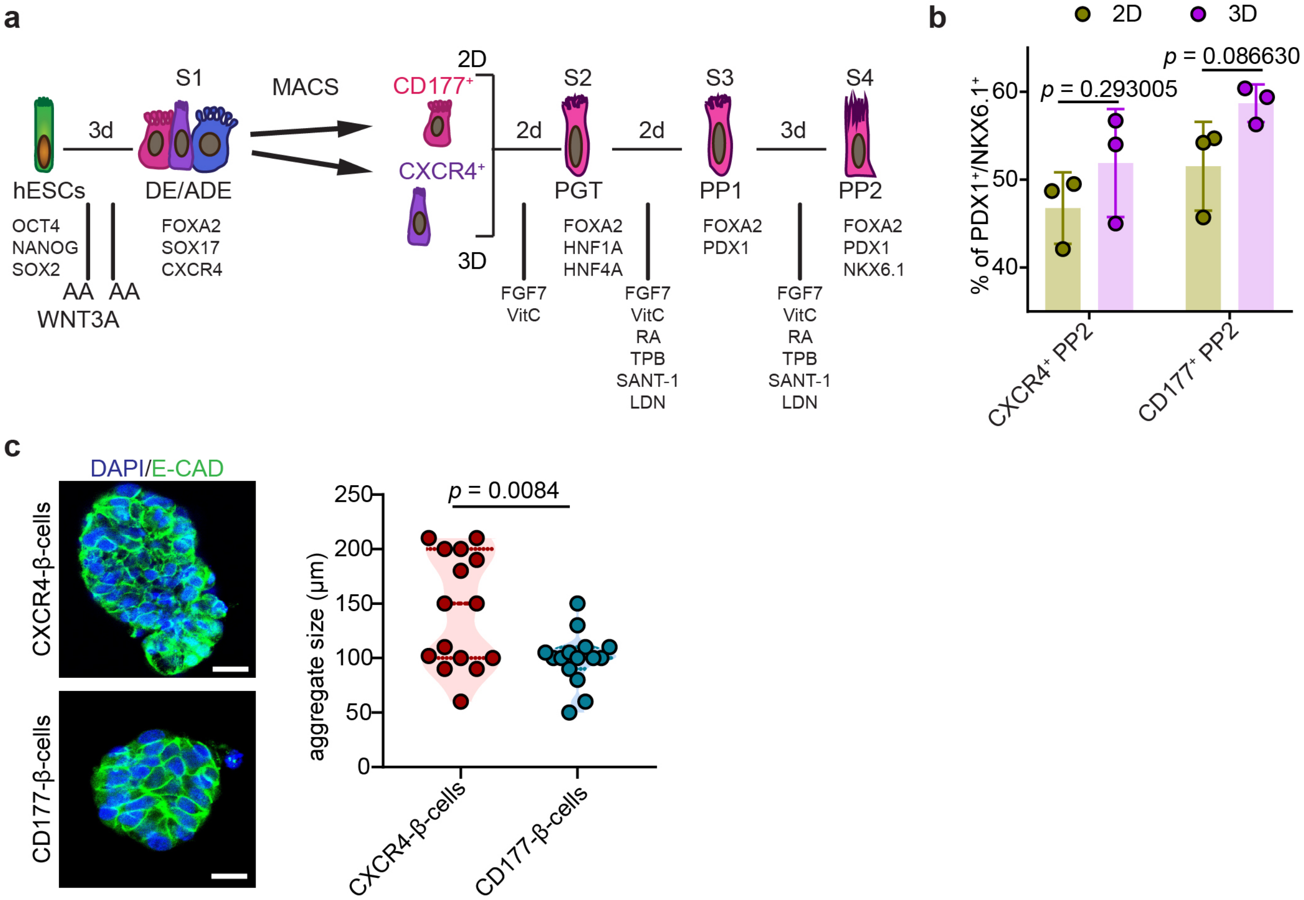

Supplementary Figure 7

Comparison of 2D and 3D culture system on pancreatic differentiation

(a) Overview of differentiation protocol used. (b) Comparison of PDX1$^+$/NKX6.1$^+$ generated from CD177$^+$- and CXCR4$^+$-ADE in 2D and 3D settings (two-sided unpaired Student's *t*-test, *n* = 3 biologically independent experiments). (c) Morphology of CD177- and CXCR4-β-cells; DAPI (blue) and E-CAD (green). Scale bars, 20 µm. Graph represents the size of the aggregates in µm (two-sided unpaired Student's *t*-test, *n* = 15 aggregates from 3 biologically independent experiments). Data is represented as mean ±s.e.m, P<0.05. Statistically non-significant results are not indicated in the figure.

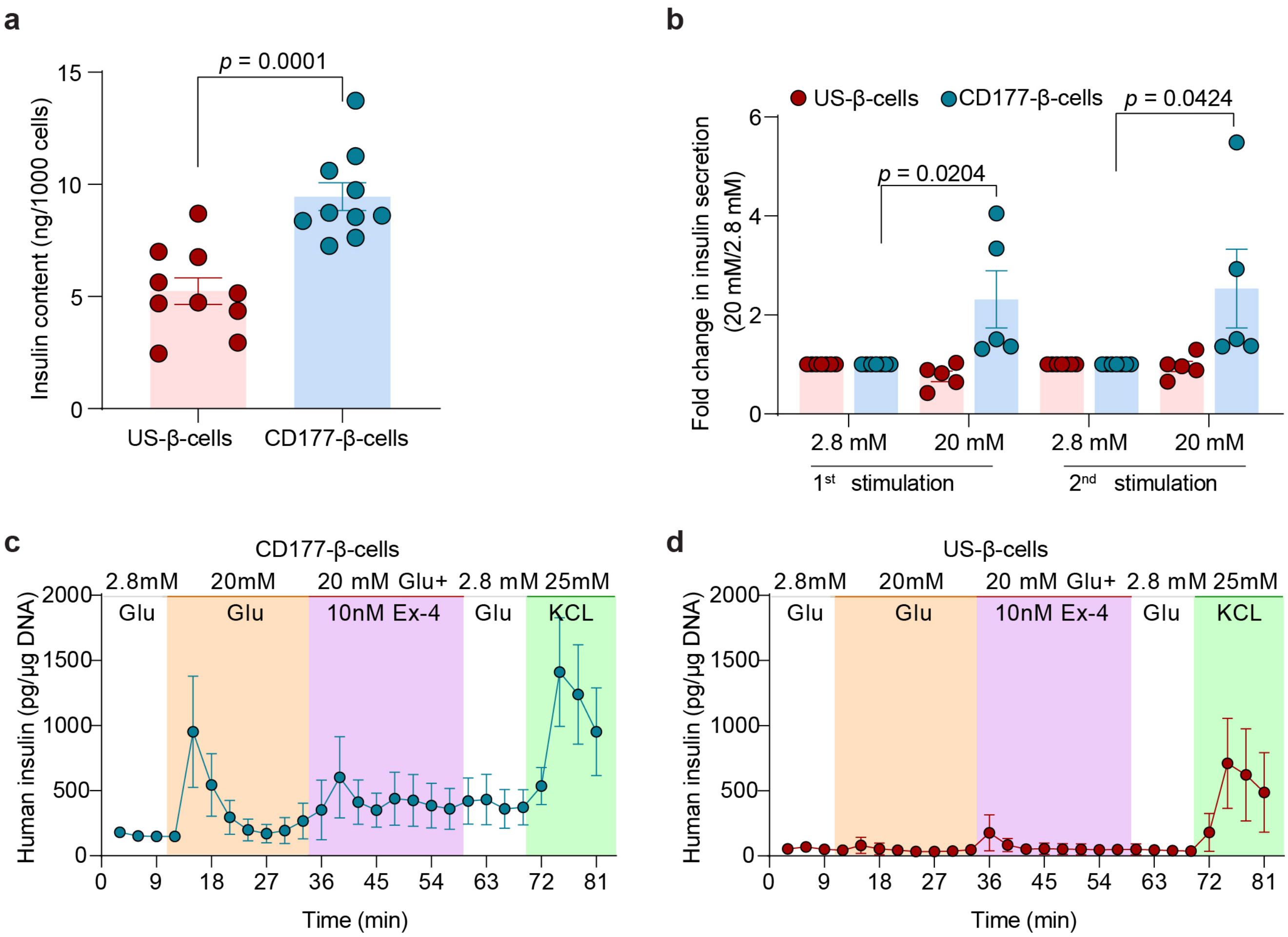

Supplementary Figure 8

H1 hESC-derived CD177^{+}-ADE generates more functional β-like cells *in vitro*

(a) Insulin content of US-β-cells and CD177-β-cells (two-sided unpaired Student's *t*-test, *n* = 10, biologically independent experiments). (b) Comparison of insulin secretion of US-β-cells and CD177-β-cells in sequential static GSIS (two-sided unpaired Student's *t*-test, *n* = 5, biologically independent experiments). (c,d) Insulin secretion in response to dynamic glucose, Ex-4 and KCl challenges in a perifusion system on US-β-cells (c) and CD177-β-cells (d) ((c,d) n = 5, biologically independent experiments). Data is represented as mean ±s.e.m; P<0.05 and P<0.01. Statistically non-significant results are not indicated in the

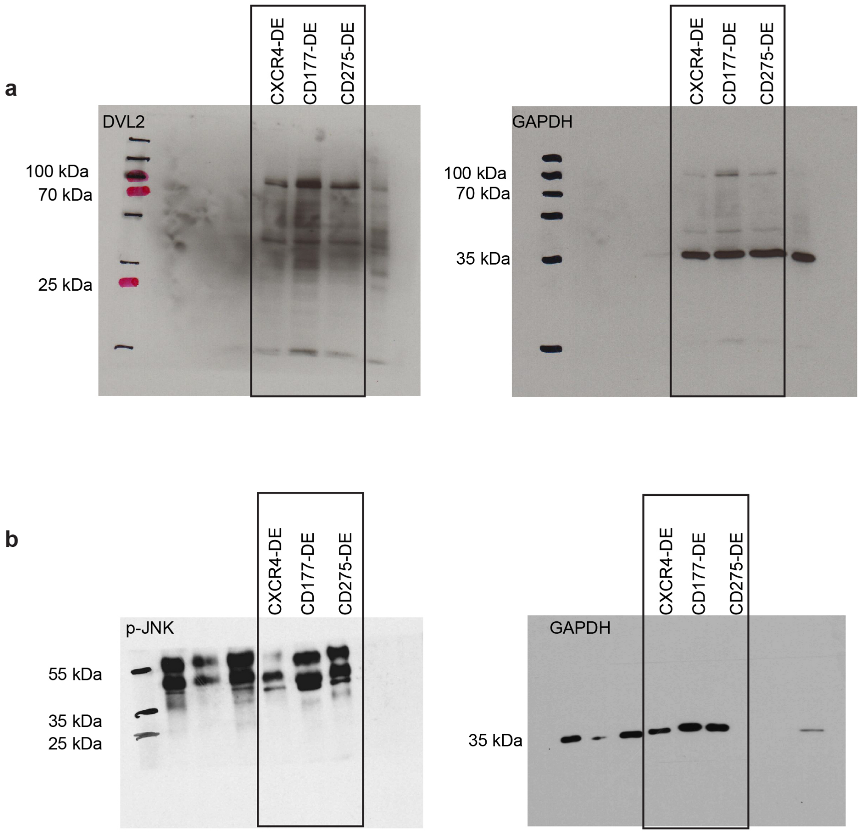

Supplementary Figure 9

CD177$^+$ and CD275$^+$ ADE receive differential Wnt signalling

(a,b) Original Western blot of WNT/PCP components such as DVL2 (a) and p-JNK (b) in ADE subpopulations as shown in Figure 2h.

Supplementary Table 1: List of antibodies selected for secondary screen

No	**Antibody**	**Isotype**
1	CD44	Mouse IgG1
2	CD90	Mouse IgG1
3	CD111	Mouse IgG1
4	CD133/1 (AC133)	Mouse IgG1
5	CD146	Mouse IgG1
6	CD262	Mouse IgG1
7	CD275 (B7-H2)	Mouse IgG1
8	Anti-PTK7 (CCK-4)	Mouse IgG2a
9	CD133/2 (293C3)	Mouse IgG2b
10	Anti-PSA-NCAM	Mouse IgM
11	CD15	Mouse IgM
12	CD49f	Rat IgG2a
13	ANTI CX3CR1	Rat IgG2b
14	Anti CCR10	Recombinant human IgG1
15	Anti HLA-DQ	Recombinant human IgG1
16	Anti-SSEA1	Recombinant human IgG1
17	Anti- SSEA4	Recombinant human IgG1
18	CD46	Recombinant human IgG1
19	CD47	Recombinant human IgG1
20	CD49b	Recombinant human IgG1
21	CD51	Recombinant human IgG1

22	CD82	Recombinant human IgG1
23	CD131	Recombinant human IgG1
24	CD138 (44F9)	Recombinant human IgG1
25	CD171 (LCAM)	Recombinant human IgG1
26	CD177	Recombinant human IgG1
27	CD244 (2B4)	Recombinant human IgG1
28	CD270 (HVEM)	Recombinant human IgG1
29	DCIR	Recombinant human IgG1
30	CD234	Recombinant human IgG1

Supplementary Table 2: Stage-wise comparison of pancreatic progenitors and β-like cells (S3-S7) generated from enriched CD177$^+$ ADE and CXCR4$^+$ ADE vs already published protocols*.

Stage (% of cells from total population)	**CD177$^+$ derived pancreatic precursors**	**CXCR4$^+$ derived pancreatic precursors**	**Bulk differentiation according to Rezania et.al., 2014 (as published)**	**Bulk differentiation according to Pagliuca et.al., 2014 (as published)**
S3: PDX1$^+$ cells	>70%	>50%	>89%	>85%
S4: PDX1$^+$/NKX6.1$^+$	>60%	>50%	>62%	>55%
S6: **INS$^+$/NKX6.1$^+$** **GCG$^+$/INS$^+$**	>60% >13%	>50% >10%	>44% >20%	**C-peptide$^+$/NKX6.1$^+$:** >38% **GCG$^+$/C-peptide$^+$:** >8%
S7: **INS$^+$/MAFA$^+$** **INS$^+$/GLUT1$^+$**	>30% >30%	>20% >20%	NA NA	NA NA

Supplementary Table 3: List of primers for qPCR

Primer	Sequence/TaqMan id
GAPDH	Hs02758991_g1
18S	Hs99999901_s1
FOXA2	Hs00232764_m1
SOX17	Hs00751752_s1
CER1	Fwd: CCCATCAAAAGCCATGAAGT Rev: TTTCCCAAAGCAAAGGTTGT
HHEX	Fwd: ACGGTGAACGACTACACGC Rev: CTTCTCCAGCTCGATGGTCT
CELSR1	Hs00947712_m1
WNT4	Hs01573504_m1
WNT5A	Hs01086864_m1
DVL2	Hs00182901_m1
WNT3A	Hs00263977_m1
AXIN2	Hs00610344_m1
NGN3	Hs01875204_s1
PDX1	Hs00236830_m1
NKX6.1	Hs01055914_m1
NEUROD1	Hs01922995_s1
MAFA	Hs01651425_s1/Hs04186804_s1
GLUT1	Hs00892681_m1
UCN3	Hs00846499_s1
TTR	Fwd: ACTTGGCATCTCCCCATTC Rev:TAGGAGTAGGGGCTCAGCAG
AFP	Hs00173490_m1
NKX2.2	Hs00159616_m1

INS	Hs02741908_m1
GCG	Hs01031536_m1

Supplementary Table 4: List of Antibodies for Immunohistochemistry, FACS and Western blotting

Conjugated antibodies:

Antibody	Company	Catalogue No	Dilution FACS
Human CXCR4-PE Human CXCR4-APC	Miltenyi Biotec Miltenyi Biotec	130-098-354 120-010-802	1:40
Human CD117-APC Human CD117-PE	Miltenyi Biotec Miltenyi Biotec	130-091-733 130-091-734	1:40
FOXA2 Alexa Fluor® 488	R and D	IC2400G	1:10
SOX17 APC	R and D	IC1924A	1:10
Human CD177-APC	Miltenyi Biotec	120-017-498	1:20
Human CD275-APC	Miltenyi Biotec	120-012-112	1:20
PE Mouse anti-PDX1	BD Pharmingen™	562161	1:40
Alexa Fluor® 647 Mouse anti-Nkx6.1	BD Pharmingen™	563338	1:40
Alexa Fluor® 647 Mouse IgG1 κ Isotype Control	BD Pharmingen™	563023	1:40

Unconjugated antibodies:

Antibody	**Company**	**Catalogue No**	**Dilution FACS**	**Dilution IF**
Rabbit FOXA2	Cell signalling	8186	1:1000	1:1000
Goat SOX17	Acris/Novus	GT15094	1:1000	1:1000
Goat CER1	R&D Systems	AF1075	1:1000	1:1000
Mouse β-catenin	BD	610154	1:1000	1:1000
Guinea pig INSULIN	Thermo Scientific	PA1-26938	1:100	1:100
Guinea pig C-peptide	Abcam	ab30477	1:300	1:300
Rabbit MAFA	Betalogics	LP9872	1:100	1:100
Rabbit MAFA	Novus Biologicals	NB400-137	1:100	1:100
Rabbit GLUT1	Thermo Fisher	PA1-37782	1:100	1:100
Goat GATA6	R&D Systems	AF1700	1:1000	1:1000
Mouse SOX2	Abgent / Bio Cat	AM2048	1:1000	1:1000
Rabbit CDX2	Santa Cruz	sc-134468	1:1000	1:1000
Mouse GCG	Sigma	G2654-.2ML	1:300	1:300
Goat PDX1	R&D Systems	AF2419	1:100	1:500
Rabbit NKX6.1 Goat NKX6.1	Novus biologicals R&D systems	NBP1-49672 AF5857	1:200 1:300	1:500 1:300

Unconjugated antibodies:

Antibody	**Company**	**Catalogue No**	**Dilution**
Rabbit p-JNK	Cell signalling	4668	1:1000
Rabbit DVL2	Cell signalling	3216	1:1000
Mouse β-catenin	BD	610154	1:2000
Mouse GAPDH	Merck Biosciences	CB1001	1:6000